

# Peripheral somatosensory fMRI in mouse at 11.7 T

Eric T. Ahrens<sup>1\*</sup> and David J. Dubowitz<sup>2</sup>

<sup>1</sup>Department of Biological Sciences, Pittsburgh NMR Center for Biomedical Research, Carnegie Mellon University, Pittsburgh, PA 15213-2683, USA

<sup>2</sup>Department of Biology, California Institute of Technology, Pasadena, CA 91125, USA

Received 11 January 2001; revised 7 March 2001; accepted 5 April 2001

**ABSTRACT:** The feasibility of performing extremely-high resolution somatosensory fMRI in anesthetized mice using BOLD contrast at 11.7 T was investigated. A somatosensory stimulus was applied to the hindlimb of an  $\alpha$ -chloralose anesthetized mouse resulting in robust ( $p < 4 \times 10^{-3}$ ) BOLD changes in somatosensory cortex and large veins. Percentage modulation of the MR signal in cortex exceeded 7%. Experiments that artificially modulated the inspired oxygen tension were also conducted; the results revealed large, heterogeneous, BOLD contrast changes in the mouse brain. In addition,  $T_1$ ,  $T_2$ , and  $T_2^*$  values in gray matter at 11.7 T were evaluated. Discussion of the sensitivity limitations of BOLD fMRI in the tiny mouse central nervous system is presented. These methods show promise for the assessment of neurological function in mouse models of CNS injury and disease. Copyright © 2001 John Wiley & Sons, Ltd.

**KEYWORDS:** fMRI; BOLD; mouse; brain; somatosensory

## INTRODUCTION

The proliferation of genetically altered mouse strains, particularly those that resemble models of human neurological disease, has stimulated the development of methods to non-invasively assay mouse neuronal function. Towards this goal, we explore extremely high-resolution MRI, or magnetic resonance microscopy (MRM), as a means of probing mouse neurofunction. MRM is proven to be highly effective in visualizing fine structures of the mouse central nervous system (CNS) in both fixed<sup>1–4</sup> and *in vivo*<sup>5,6</sup> subjects.

Functional MRI (fMRI) has emerged as a powerful tool for investigating functional organization in the mammalian brain.<sup>7</sup> fMRI does not detect neuronal activation directly, but instead probes secondary changes; these include regional changes in cerebral blood volume (CBV), cerebral blood flow (CBF), and blood oxygenation, which give rise to the widely used BOLD (blood-oxygen-level-dependent) contrast mechanism.<sup>8</sup> BOLD contrast originates from regional perturbations in the

magnetic susceptibility of brain tissue due to changes in the relative amounts of oxyhemoglobin to deoxyhemoglobin in the capillary bed, venules and veins. These perturbations strongly impact the MR parameters  $T_2$  and  $T_2^*$  because deoxyhemoglobin is paramagnetic, whereas oxyhemoglobin is diamagnetic.<sup>9</sup> The relationship between changes in oxidative metabolism by activated neurons and the regional recruitment of excess blood oxyhemoglobin is an active area of investigation.<sup>7,10</sup>

Although several groups have reported BOLD activation in rats,<sup>11–18</sup> mice are roughly an order of magnitude smaller in size. Consequently, extremely-high signal-to-noise ratio (SNR) and resolution imaging capabilities are required, and this necessitates working at extremely high magnetic field strengths. In addition, anesthesia is required to immobilize the animals; however, its effects must not render cortical activity quiescent. Furthermore, reproducibility of the fMRI response demands that mouse physiology remain stable.

In this paper we investigate the feasibility of examining functional activation in anesthetized mice using MRM and intrinsic BOLD contrast mechanisms. These experiments were conducted at 11.7 T. First, we describe the results of *in vivo* measurements of the key magnetic resonance parameters  $T_1$ ,  $T_2$ , and  $T_2^*$  in the mouse brain. Knowledge of these parameters allows for optimum BOLD imaging. Next, we describe experiments demonstrating that the magnitude of BOLD contrast in the mouse brain can reach dramatic levels at 11.7 T; these experiments involved artificial modulation of the inspired oxygen tension. From these data, a map of the relative

\*Correspondence to: E. T. Ahrens, Carnegie Mellon University, 4400 Fifth Ave, Pittsburgh, PA 15213-2683, USA.

Email: eta@andrew.cmu.edu

Contract/grant sponsor: National Multiple Sclerosis Society; contract grant number: RG3071A1/1.

Contract/grant sponsor: National Institutes of Health; contract grant number: DA 08944, RR 13625, MH 61223, RO1 EY11933.

Contract/grant sponsor: National Science Foundation; contract grant number: CCR-0086065.

**Abbreviations used:** BOLD, blood-oxygen-level-dependent; EPI, echo planar imaging; SE, spin echo; SNR, signal-to-noise ratio.

sensitivity of various brain regions to controlled changes in blood oxygenation was derived. We then describe fMRI experiments in which a periodic somatosensory stimulus was applied to the mouse hindlimb. Correlated functional maps were obtained indicating localized neuronal activation within cortical regions. Significant activation was also observed within large draining veins in subarachnoid regions. Our results demonstrate some of the limitations of using BOLD imaging for mouse-sized subjects at extremely high magnetic field strengths. We discuss these limitations in terms of the relationships among the size of the neuro-anatomical functional unit, the SNR, and the spatial/temporal resolution.

## EXPERIMENTAL

### MRM instrumentation

Image data were acquired using a Bruker AMX 500 micro-imaging system (Bruker Instruments Inc., Billerica, MA) with a 89 mm vertical bore 11.74 T magnet. An optimized laboratory-built 1 cm diameter surface coil imaging probe was utilized for the BOLD contrast imaging and the  $T_2^*$  measurements. This probe incorporates a stereotaxic head restraint in order to limit head motion and a mask that loosely fits over the animal's nose and mouth to administer inhalation gases. A 30 mm diameter birdcage volume coil was used for the  $T_1$  and  $T_2$  measurements in order to ensure a homogeneous RF refocusing pulse. The mouse temperature was regulated at 37°C using a temperature regulated collet surrounding the animal connected to a closed-cycle water bath. These studies were conducted at the Biological Imaging Center at the California Institute of Technology, Pasadena, CA and were approved by the Institutional Animal Care and Use Committee.

### MR relaxation times in the *in vivo* mouse brain

Maps of the relaxation times  $T_1$ ,  $T_2$  and  $T_2^*$  were calculated within a single coronal brain slice. Adult female mice (~19 g, C57BL) were anesthetized using an intraperitoneal (i.p.) injection of a cocktail containing ketamine (0.07 mg/g) and xylazine (0.004 mg/g). The mouse was then mounted into the imaging probe and positioned into the magnet bore. After approximately 30 min, gaseous isoflurane (0.6 % in air) was administered *in situ* in order to maintain the mouse under light anesthesia for the duration of the imaging session.

The  $T_1$  and  $T_2$  data were acquired using a saturation-recovery two-dimensional Fourier transform (2DFT) spin-echo protocol. All measurements were made on a single coronal brain slice. For  $T_1$ , seven images were collected with  $TR$  ranging from 0.3 to 13 s and  $TE = 8$  ms. The  $T_2$  was obtained using ten single-echo images with

$TE$  values ranging from 4.5 to 90 ms and  $TR = 10$  s. The  $T_2^*$  values were obtained using the same surface coil probe used for the fMRI experiments and using a 2DFT gradient-echo protocol using one line of  $k$ -space per excitation and a small tip-angle RF pulse; the  $TE$  values were varied in 10 steps ranging from 4.5 to 50 ms and  $TR = 50$  ms. Field shimming was performed manually on the image slice. This was performed by turning off the read-out gradient and manually maximizing the integrated echo intensity by adjusting the shim currents on the eight lowest-order shims (based on the spherical harmonics). All data were acquired with  $128 \times 128$  image points and a resolution of 117  $\mu\text{m}$  in-plane, with a slice thickness of 1.5 mm.

For each data set we used a voxel-wise least squares fitting routine. The appropriate single-exponential recovery functions for  $T_1$ ,  $T_2$ , and  $T_2^*$  were utilized.<sup>19</sup> From the maps of calculated relaxation times, regions of interest (ROI) were defined to obtain average relaxation time values in various brain regions. All measurements were repeated using the above procedures for  $n = 4$  mice.

### Characterizing BOLD contrast by modulation of inspired oxygen tension

Mice were anesthetized and prepared for imaging using the same methods as described above. Blood oxygen was modulated by alternating the inhalation gas between 100%  $\text{O}_2$  and a mixture of 10%  $\text{O}_2$ /90%  $\text{N}_2$ . Previous studies<sup>20</sup> have shown that this gas combination perturbs the CBV and CBF by only a small amount (~10%). We assumed that the observed intensity changes are primarily due to modulation of blood-oxygenation, and we ignored small contributions from CBV and CBF to the overall BOLD signal. Each gas was delivered for a period of 1 min, and the gases were alternated for five cycles.

Gradient-echo images were acquired continuously within a single coronal brain slice during the five gas cycles. Images were primarily  $T_2^*$ -weighted, and multiple experimental runs were performed at various  $TE$  values ranging from 4.5 to 12 ms. A small tip-angle excitation pulse (~3°) was utilized with  $TR = 60$  ms, two  $k$ -space averages, and an imaging time of 15 s per slice. Thus, four imaging slices were acquired for each 1 min gas exposure, or eight time-points per complete cycle. The image resolution was 98  $\mu\text{m}$  in-plane, with a 1.0 mm slice thickness. These experiments were repeated in  $n = 4$  mice. Anatomical images were acquired using a 2DFT gradient-echo protocol with  $TR/TE = 60/5.4$  ms, an in-plane resolution of 98  $\mu\text{m}$ , and a 1.0 mm slice thickness. The shimming method followed the same protocol used in the relaxation-time experiments.

The time-dependent image data were processed off-line using AFNI software.<sup>21</sup> In order to pick out voxels exhibiting significant intensity changes due to hypoxia, we performed a voxel-by-voxel cross-correlation analy-

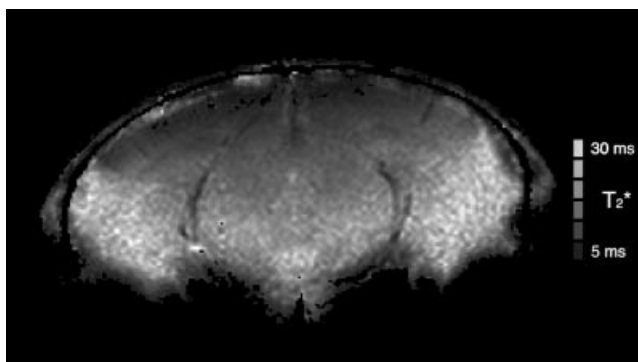


**Figure 1.** Calculated  $T_2^*$  map through a coronal brain slice. Data were acquired using a 2DFT gradient-echo sequence with a small tip-angle RF pulse; the  $TE$  values were varied in 10 steps ranging from 4.5 to 50 ms and  $TR = 50$  ms. Resolution is  $117 \mu\text{m}$  in-plane, with a slice thickness of 1.5 mm. Note the large  $T_2^*$  heterogeneity observed across the slice

sis. A linear fit function of the form

$$x(t) = ar(t) + b \quad (1)$$

was used, where  $x(t)$  is the time-dependent voxel intensity,  $r(t)$  is a trapezoidal model intensity function (or 'stimulus' waveform),  $a$  is the fit coefficient,  $b$  is the baseline intensity in the hypoxic state, and  $t$  is time. The trapezoid model varied from 0 to 1 in amplitude, with a period of eight time periods and one time period allotted to ramp up or down. To remove spurious pixels, the functional intensity map was threshold at a correlation-coefficient value of  $|r| > 0.5$  (uncorrected  $p < 0.01$ ). A map of the percent image intensity changes, given by  $\Delta I = (a/b) \times 100\%$ , was calculated and superimposed onto the anatomical image using AFNI. A rainbow color scale was used to represent the magnitude of the percent change ( $\Delta I$ ).

## fMRI

Adult mice ( $\sim 19$  g, strain C57BL) were anesthetized with gaseous isoflurane (1.5% in 100%  $\text{O}_2$ ). After approximately 10 min an i.p. injection of  $\alpha$ -chloralose was administered (0.08 mg/g) while under isoflurane anesthesia. After an additional 20 min the isoflurane was removed and the mouse was mounted into the surface coil imaging probe.

Two electrodes consisting of a single turn of fine copper wire coated with conductive jelly were wound around the hind paw in order to apply a small somatosensory electrical stimulation ( $\sim 50 \mu\text{A}$ ). The periodic stimuli consisted of five 65 s pulses of 3 Hz stimulation interspersed by 'off' periods of the same duration. The stimuli were far below the threshold needed to induce a visible motor response. A computer running a

Labview software program (National Instruments Inc., Austin, TX) was used to orchestrate the stimulus and image acquisitions.

Para-sagittal images were acquired on a single slice offset approximately 2 mm from the midline using a gradient-echo method. The imaging parameters were  $TR/TE = 17/7$  ms,  $64 \times 64$  image points, an in-plane image resolution of  $180 \mu\text{m}$ , a 1.5 mm-thick slice, and 10 averages. The  $TE$  value was set to approximately the measured value of  $T_2^*$  in cortex (see the next section). The total imaging time for a single slice was approximately 11 s. Images were acquired continuously throughout the on and off stimulus periods. Spin-echo  $T_2$ -weighted anatomical images were acquired with  $TR/TE = 1200/34$  ms, an in-plane resolution of  $45 \mu\text{m}$ , and a 1.5 mm slice thickness. Shimming followed the same protocol described earlier.

The time-dependent data were processed off line using a linear fit [Eqn (1)] and the AFNI analysis software described above. Functional images were generated using a cross-correlation technique.<sup>22</sup> A series of phase-shifted trapezoids were used as the model stimulus reference waveforms; these were cross-correlated on a voxel-by-voxel basis with the MR signal time-course. A hot-body color scale was used to represent the MR signal % change. Spurious pixels were removed with a threshold set at a correlation-coefficient value of  $|r| > 0.6$  ( $p < 4 \times 10^{-3}$  following a conservative Bonferroni correction for multiple comparisons). The anatomical image and the functional maps were co-registered using AFNI.

## RESULTS

### MR relaxation times in the *in vivo* mouse brain

From the maps of  $T_1$ ,  $T_2$ , and  $T_2^*$ , ROI were defined in cortical gray matter in order to determine mean values. The results are  $T_1 = 1.9 \pm 0.1$  s,  $T_2 = 31.4 \pm 1.1$  ms, and  $T_2^* = 7\text{--}28$  ms. These results represent average values over ROIs containing approximately 50 voxels. For  $T_1$  and  $T_2$ , the uncertainty represents the standard deviation of the mean for  $n = 4$  subjects. A calculated map of the  $T_2^*$  values through a coronal slice is displayed in Fig. 1. A substantial amount of  $T_2^*$  heterogeneity is observed, with values tending to increase smoothly in a dorsal-ventral fashion; values of order of 7 ms were observed near the dorsal-most cortical regions and increase to  $\sim 28$  ms in ventral brain regions.

### BOLD contrast by modulation of oxygen tension

Plate 1 shows a coronal map of the percent changes in image intensity ( $\Delta I$ ) resulting from changes in blood oxygenation. Intensity changes in brain parenchymal

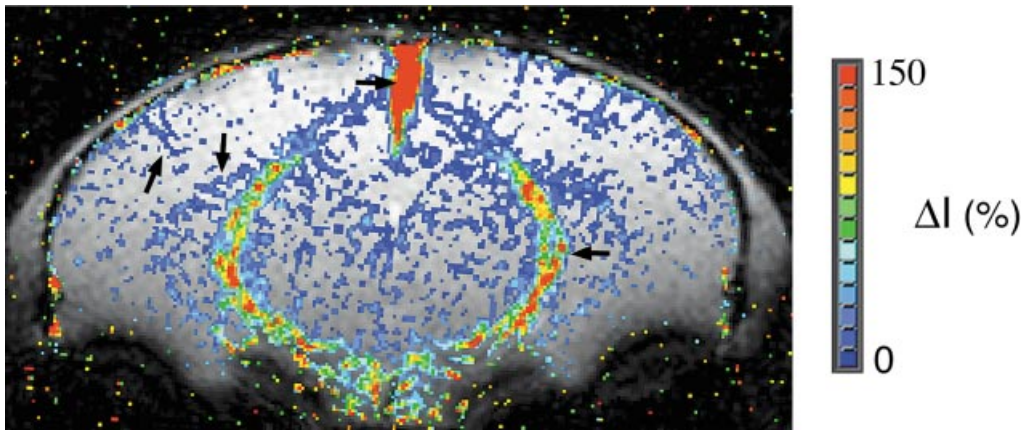


**Plate 1.** Coronal brain map of BOLD intensity changes due to hypoxia. Shown is a map of the percentage intensity changes calculated from  $\Delta I = (a/b) \times 100\%$  [see text and eqn (1)] and displayed in rainbow scale; the map is superimposed onto an anatomical image. These results demonstrate the heterogeneity of BOLD contrast in the brain and the potential high-sensitivity of this mechanism at 11.7 T. Blood-oxygen content was modulated in an anesthetized mouse by alternating the inhalation gas between 100% O<sub>2</sub> and a mixture of 10 %O<sub>2</sub>/90% N<sub>2</sub>. T<sub>2</sub>\*-weighted gradient-echo images were acquired continuously during multiple gas cycles. These data were acquired with  $TR/TE = 60/6.8$  ms, 98 μm in-plane resolution, and a 1 mm slice thickness. A cross-correlation analysis was used to threshold only those voxels exhibiting significant intensity changes (uncorrected  $p < 0.01$ ). Data were overlaid onto an anatomical image acquired in the same image plane. Substantial changes are observed in large draining veins, arteries, and parenchymal tissue. Black arrows indicate (from left to right) capillary networks in cortex and hippocampal regions, the sagittal sinus, and pial vessels

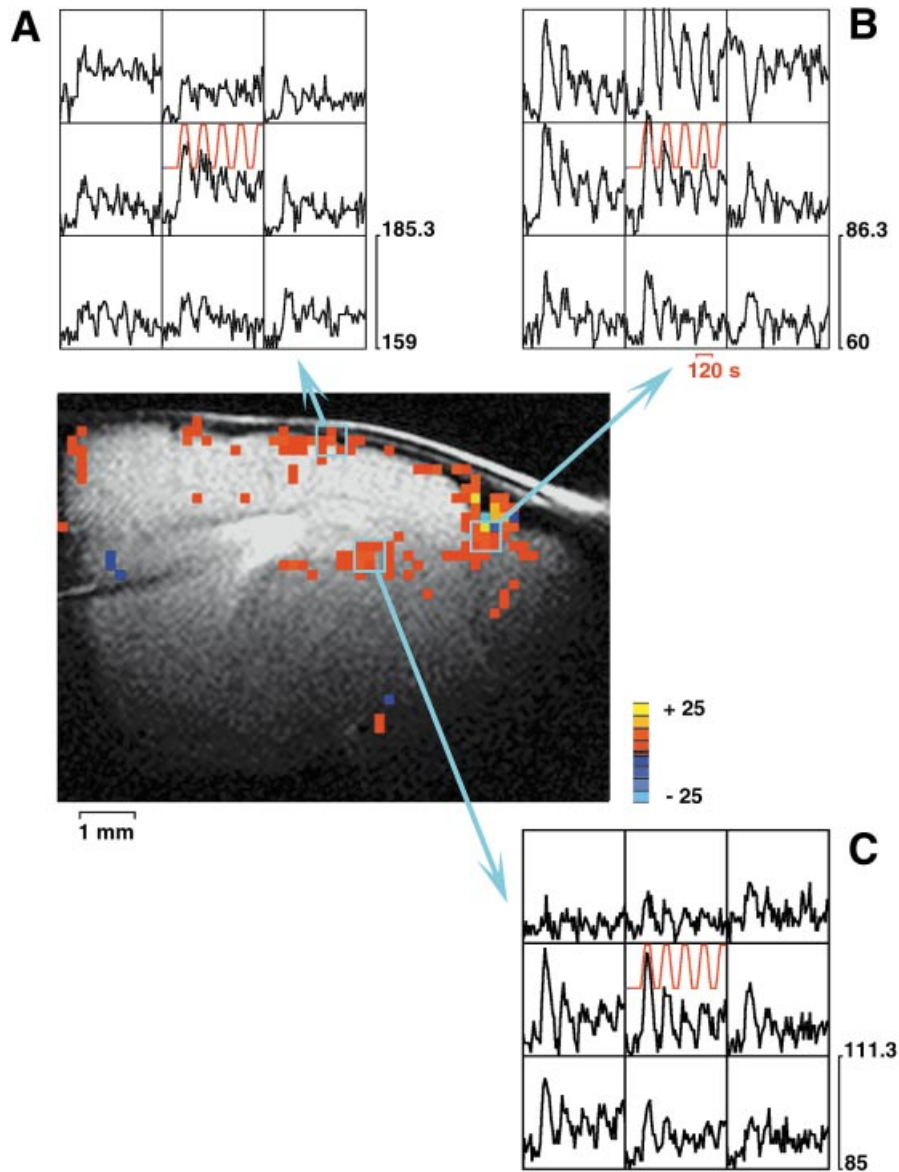


**Plate 2.** fMRI map in the mouse brain resulting from a somatosensory stimulus to the hindlimb. The fMRI map (center panel) is overlaid onto a para-sagittal anatomical image. The slice is contralateral to the stimulated side. There is strong activation (corrected  $p < 4 \times 10^{-3}$ ) in somatosensory regions and in large draining veins. (a–c) The time course of the voxel intensities of the raw data for various ROI. Shown are the somatosensory cortex (a) and large draining veins (b–c). The model stimulus function is drawn in the middle frame of each panel. The percentage modulation of the MR signal in the ROI are approximately 7, 20 and 15% for the somatosensory cortex, transverse sinus, and draining vein, respectively

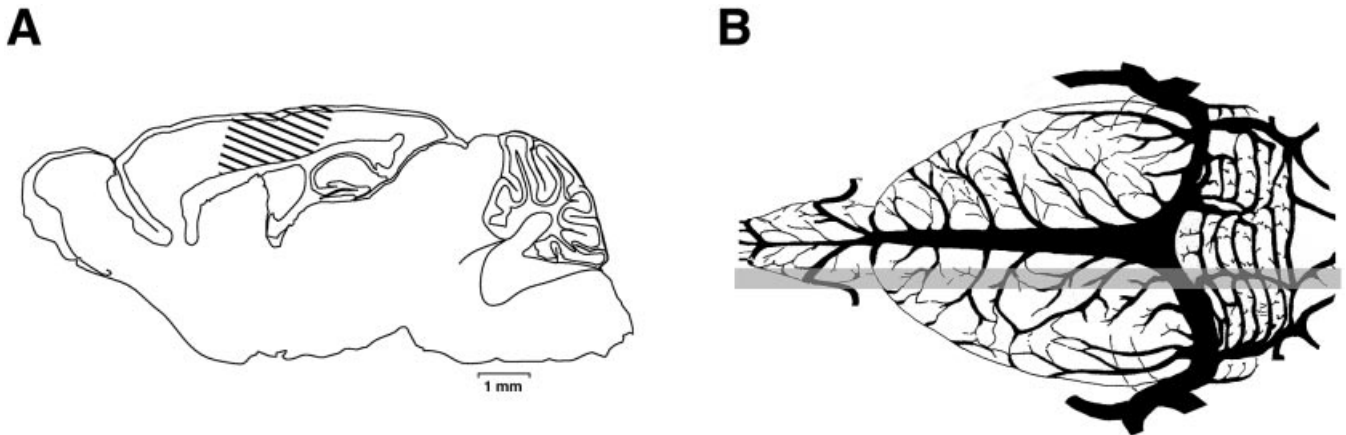


**Figure 2.** Anatomy of mouse brain. (a) A diagram of a para-sagittal cross-section. The limb somatosensory cortical regions are shaded. (b) A dorsal view of the superficial venous system of a mouse. The approximate location of the image slice shown in Plate 2 is indicated in (b) by a shaded bar. [Figure 2(b) is adapted from Paxinos.<sup>41</sup>]

tissue are of order of 10–20%. Prominent signal changes are observed in proximity to large vessels, especially the sagittal sinus (~150%).

## fMRI

Plate 2 (center panel) shows a map of voxels exhibiting stimulus-correlated intensity changes; a para-sagittal anatomical image is also superimposed. The functional map shows robust activation ( $p < 4 \times 10^{-3}$ , corrected for multiple comparisons) in somatosensory cortex. Large draining veins in subarachnoid regions also exhibit a substantial modulation in intensity. The data shown are on the side contralateral to the stimulus. Data on the ipsilateral side (not shown) shows no significant activation.

Plate 2(a–c) displays the time course of voxel intensities for various ROI. Shown are the somatosensory cortex (a), the transverse sinus (b), and the sagittal sinus (c). The model stimulus function is indicated by the solid red trace in the middle frame of each panel. The percentage modulations of the ROI intensities were approximately 7, 20 and 15% for the somatosensory cortex, transverse sinus and sagittal sinus, respectively. These values were calculated from  $\Delta I = (a/b) \times 100\%$ , where the parameters were obtained from the model fit of data [described by eqn (1)].

For reference, Fig. 2(a–b) shows schematic diagrams of various aspects of mouse brain anatomy. Figure 2(a) shows a para-sagittal tracing in approximately the same location as the fMRI slice shown in Plate 2. The primary somatosensory areas are indicated. Figure 2(b) shows a dorsal view of the mouse superficial venous system; the approximate location of the fMRI slice of Plate 2 is indicated by a shaded bar. Note that the image plane intersects several large draining veins, especially the

transverse sinus, which shows up in the correlation map (Plate 2).

## DISCUSSION

### Relaxation times

The first step in the optimization of fMRI in mouse is the characterization of the longitudinal relaxation times  $T_1$ ,  $T_2$ , and  $T_2^*$  in the brain which are magnetic field strength-dependent and may depend on species. The most important parameter for gradient-echo BOLD contrast imaging is  $T_2^*$  in parenchyma, where setting  $TE \approx T_2^*$  maximizes the contrast-to-noise ratio.<sup>23</sup> The measured values of  $T_2^*$  varied by a factor of four (7–28 ms) across the brain slice (Fig. 1). Presumably this heterogeneity is due to discontinuities in the magnetic susceptibility among different materials (i.e. air/bone/brain)<sup>24</sup> that give rise to macroscopic magnetic field gradients that cannot be removed with shimming. The spin-dephasing contribution to  $T_2^*$  due to susceptibility gradients is accentuated by working at extremely-high magnetic fields.<sup>24</sup> In our fMRI and blood gas experiments,  $TE$  was set to a value of  $\sim 7$  ms, which is approximately the  $T_2^*$  value observed in the somatosensory cortex regions. The longest  $T_2^*$  values ( $\sim 28$  ms) were observed in regions near the basal ganglia and are comparable to  $T_2$  in parenchyma (31.4 ms).

The value of  $T_2 = 31.4$  ms measured in parenchyma is significantly less than values obtained in other species at lower fields. For example,  $T_2$  values in rat and cat gray matter at 9.4 and 4.7 T are reported to be 40 and 50 ms, respectively,<sup>12,25</sup> and in humans  $T_2 = 101$  ms at 1.5 T.<sup>26</sup> Interestingly, at 11.7 T the ratio of  $T_1/T_2 = 60.5$  is exceedingly large; by comparison,  $T_1/T_2 = 9$  at 1.5 T (in human gray matter).<sup>26</sup> Because the imaging time increases monotonically with the parameter  $T_1/T_2$ ,<sup>27</sup> this

observation highlights one of the fundamental difficulties associated with the implementation of rapid-imaging methods at extremely-high magnetic field strengths.

### Modulation of oxygen tension

In order to investigate the sensitivity and spatial distribution of apparent BOLD effects in the mouse brain at 11.7 T, we investigated image changes in response to the modulation of the inspired oxygen tension; the combination of gases used minimizes perturbations in CBF and CBV.<sup>20</sup> Theoretical analysis suggests that  $T_2^*$  and BOLD-contrast changes in proximity to vessels are strongly dependent on magnetic field strength.<sup>28</sup>

Using the inhalation gas assay, the magnitude of BOLD intensity changes in parenchyma are at the 10–20% level and of order 150% in large vessels (Plate 1). Changes in parenchyma are presumably due to blood-oxygenation variations in the capillary bed. We note that the potential intensity changes may in fact be significantly larger than what we have described for two reasons. First, the changes in parenchyma did not completely saturate to a constant value after 1 min exposure to hypoxic conditions. [This is in contrast to the large vessels (*e.g.* sagittal sinus) where intensity changes saturated in <20 s.] Exposure to hypoxic conditions was not continued beyond 1 min in order to avoid harming the animal. Second, the experiments were repeated for a range of  $TE$  values, but due to the shortness of  $T_2^*$  in dorsal-most brain regions only the  $TE = 6.8$  ms data was used to ensure adequate SNR throughout the slice for the cross-correlation analysis; this  $TE$  value does not optimize the BOLD changes in all brain regions.

### fMRI

The intent of these studies was to determine whether BOLD contrast fMRI is effective in analyzing mouse neurofunction. The results show significant cortical activation at the 7% level in limb somatosensory cortex (Plate 2); thus these methods show promise as a tool for elucidating normal neurofunction and neuropathology. We note that one other group has reported comparable magnitude BOLD signal changes in mouse in response to visual stimuli.<sup>29</sup>

Our results also bring to light several limitations of the technique. These stem from ubiquitous SNR limitations of MRI and the temporal resolution limitations associated with working at extremely high magnetic field strengths. Furthermore, the need to work with anesthetized animals and the vertical orientation of the animal in the magnet bore may impact the results.

Performing fMRI in mouse is substantially more difficult than in rat, where robust BOLD signals have

been observed by numerous groups. Consider the relative size of the cortical functional unit between these two species. Cortical somatosensory cytoarchitecture has a high degree of compartmentalization,<sup>30</sup> and there is a similar organization in mouse and rat.<sup>31</sup> For the sake of scaling arguments, consider the relative volume of a widely studied somatosensory unit, the whisker barrel cortex. From cytochrome oxidase-stained tangential sections of flattened cortex, the measured mean area ratio of mouse to rat barrels is of order of 0.2 (Woolsey TA, private communication), and an estimate of the volume ratio is of order of 0.09. Thus, the volume of the functional unit is approximately 10 times smaller in mouse than in rat, and the voxel volume needs to be approximately 10 times smaller to achieve the same degree of cortical localization. Because SNR is proportional to voxel volume, there is a substantial loss in sensitivity when attempting to resolve the mouse functional unit. Although the whisker barrel is used as an example here, we speculate that the same relative sizes apply to somatosensory limb regions.

Some of the loss in SNR can be recovered by working at a higher magnetic field strength. For example, increasing the imaging field strength from 9.4 T (the highest field fMRI results in rat reported to date) to 11.7 T provides a SNR gain of order of 50%. This assumes a  $B_0^{7/4}$ -dependence of SNR on field strength ( $B_0$ ) and all other parameters held constant.<sup>27</sup> In addition to the gains in SNR by going to higher field strength, one also gains in the sensitivity to BOLD contrast due to heightened local field gradients in proximity to vessels. Numerical simulations show the BOLD contribution to the transverse relaxation rate scales linearly with  $B_0$  for large vessels and quadratically for small vessels (compared to the voxel size).<sup>32</sup> Quantitative verification of these scaling relations in the brain is problematic due to partial volume contamination and uncertainties in numerous parameters.<sup>33</sup> Although there is a lack of quantitative data for the field strengths utilized in this study, on the basis of the theoretical estimates and extrapolation of lower field results,<sup>33</sup> going from 9.4 to 11.7 T yields an increase of less than a factor of two in the functional contrast-to-noise ratio (CNR). The upshot is that, although the image SNR (and resolution) and BOLD CNR is improved by moving to higher field strengths, the improvement may not be sufficient to offset the reduced sensitivity due to the very small size of the functional structures in mouse compared to rat.

In addition to cortical activation, the fMRI results (plate 2) show substantial correlated intensity changes in large draining veins that are distant from the activated neurons. At least two factors may play a role in this behavior. Changes in arterial and venous CBF may accompany the stimulus. This results in an 'in-flow' effect where fully magnetized spins flow into the imaging plane and modulate the image intensity in a correlated fashion. In-flow effects may also provide a contribution

to the large intensity changes observed in vessels in the blood-gas experiments (Fig. 1), although the gas combination used was designed to minimize these effects. We have made no attempt to quantify in-flow contributions in the present studies, and this is a topic of future work.

A second consideration stems from the relatively low temporal resolution ( $\sim 10$  s per image) of the fMRI data; the long acquisition times are a consequence of the high spatial resolution and the necessity for signal averaging in order to obtain satisfactory SNR. Optical studies have examined the temporal relationships between CBF, CBV, and blood oxygenation<sup>34</sup> of the BOLD response following neuronal stimulation. These studies show that the initial deoxyhemoglobin increase is well localized with the sites of elevated neuronal firing, and that the later oxyhemoglobin increase is less localized; also, increasing the stimulus duration reduces the signal-to-noise ratio of the activation maps.<sup>34</sup> Recent fMRI studies in cat<sup>35</sup> have shown that activation maps generated at different time points along a biphasic BOLD response display varying degrees of neuronal localization; maps from the initial negative dip show greater neuronal localization compared to those from the latter positive BOLD response which show substantial venous recruitment. Although a biphasic BOLD response in mouse has not been demonstrated using MRI, we speculate that mouse data acquired with better temporal resolution and with a shorter duration stimulus period may provide better localization of neuronal function and less involvement of large vessels.

Improving the temporal resolution requires implementation of rapid-imaging methods that work satisfactorily at 11.7 T. One is at a disadvantage at 11.7 T because of the large  $T_1/T_2$  ratio.<sup>27</sup> Furthermore, the shortness of  $T_2^*$  and the persistence of  $B_0$  inhomogeneities at these extreme field strengths makes implementation of artifact-free single-shot echo-planar imaging (EPI) problematic. The use of rapid spin-echo (SE) imaging methods (i.e. RARE<sup>36</sup>) may provide the best means of speeding-up acquisitions as well as reducing bulk susceptibility artifacts.<sup>37</sup> In addition, it has been suggested that SE methods are less sensitive to dephasing of large vessels and more sensitive to microvasculature.<sup>12</sup> We also note that the use of bipolar diffusion gradients to attenuate spins with high mobility in large vessels may also be useful in this regard.<sup>38</sup> These are topics for future work.

Two additional experimental considerations that may impact our results are the physiological effects of anesthesia and the vertical orientation of the mouse in the magnet bore. It is desirable to work with anesthetized animals in order to immobilize the animal and minimize stress during imaging.  $\alpha$ -Chloralose was used as the primary anesthesia for fMRI experiments because it does not significantly depress cortical activity,<sup>18</sup> provides a stable CBF,<sup>39</sup> and has been used successfully in

numerous BOLD somatosensory studies in rat. Care must be taken when using this anesthesia because there is a tendency to induce seizures after an initial injection, and thus it was administered to the animal while it was under the influence of isoflurane.

The other potential complication originates from the orientation of the animal in a vertical position within the magnet bore. Maintaining a mouse in this unnatural orientation for extended time periods may lead to physiological changes, particularly blood pressure disturbances, incomplete blood gas exchange due to respiratory difficulties, decreased cardiac output, and changes in cerebral perfusion. Furthermore, because anesthetic agents reduce vasoconstrictor tone, the adverse effects of the vertical posture may become exacerbated. Little is known about how these effects may alter the outcome of the fMRI experiment, and this area needs further investigation.

## CONCLUSIONS

We demonstrate the feasibility of peripheral somatosensory fMRI in mouse utilizing BOLD contrast mechanisms. These results are the first step in defining the spatial and temporal signatures of the BOLD effect in mouse, which is largely unknown. The refinement of these fMRI methods will permit quantitative assessment of neurological function in mouse models of CNS injury and disease, particularly those involving genetically manipulated lines; the repertoire of such techniques that are non-invasive is currently limited. Challenges remain in developing these methods for true quantitative studies. The SNR is a concern even at the extremely high magnetic field strengths used in this study. Improved methods for artifact-free rapid imaging that are suitable for working at these field strengths are also needed. In addition, new tools for the precise control of mouse physiology in the confines of the magnet bore need to be developed and refined. Finally, further exploration is necessary into the effects of various anesthesia types on mouse neurofunction.

## Acknowledgements

We thank Drs David Laidlaw, P. T. Narasimhan, Russell Jacobs and Scott Fraser for valuable comments and Carlo Quinonez for assistance with Labview programming. This work is supported in part by a grant from the National Multiple Sclerosis Society (grant RG 3071A1/1), the Human Brain Project (DA08944) with contributions from the National Institute on Drug Abuse and the National Institute of Mental Health, the NCCR (RR13625 and MH61223), the National Institutes of Health (RO1 EY11933), and the National Science Foundation (CCR-0086065).

## REFERENCES

1. Ahrens ET, Laidlaw DH, Readhead C, Brosnan CF, Fraser SE, Jacobs RE. MR microscopy of transgenic mice that spontaneously acquire experimental allergic encephalomyelitis. *Magn. Reson. Med.* 1998; **40**(1): 119–132.
2. Ahrens ET, Blumenthal J, Jacobs RE, Giedd JN. Imaging brain development. In *Brain Mapping: The Systems, Toga AW, Mazziotta JC* (eds). Academic Press: San Diego, CA, 2000; 561–589.
3. Jacobs RE, Ahrens ET, Meade TJ, Fraser SE. Looking deeper into vertebrate development. *Trends Cell Biol.* 1999; **9**(2): 73–76.
4. Benveniste H, Kim K, Zhang L, Johnson GA. Magnetic resonance microscopy of the C57BL mouse brain. *Neuroimage* 2000; **11**(6): 601–611.
5. Dubowitz DJ, Tyszka JM, Sewry CA, Moats RA, Scadeng M, Dubowitz V. High resolution magnetic resonance imaging of the brain in the dy/dy mouse with merosin-deficient congenital muscular dystrophy. *Neuromusc. Disord.* 2000; **10**(4–5): 292–298.
6. Pautler RG, Silva AC, Koretsky AP. In vivo neuronal tract tracing using manganese-enhanced magnetic resonance imaging. *Magn. Reson. Med.* 1998; **40**(5): 740–748.
7. Ogawa S, Menon RS, Kim SG, Ugurbil K. On the characteristics of functional magnetic resonance imaging of the brain. *A. Rev. Biophys. Biomolec. Struct.* 1998; **27**: 447.
8. Ogawa S, Lee TM, Kay AR, Tank DW. Brain magnetic-resonance-imaging with contrast dependent on blood oxygenation. *Proc. Natl Acad. Sci. USA* 1990; **87**(24): 9868–9872.
9. Pauling L, Coryell CD. The magnetic properties and structure of hemoglobin, oxyhemoglobin and carbonmonoxyhemoglobin. *Proc. Natl Acad. Sci.* 1936; **22**: 210–216.
10. Hoge RD, Atkinson J, Gill B, Crelier GR, Marrett S, Pike GB. Investigation of BOLD signal dependence on cerebral blood flow and oxygen consumption: the deoxyhemoglobin dilution model. *Magn. Reson. Med.* 1999; **42**(5): 849–863.
11. Burke M, Schwindt W, Ludwig U, Hennig J, Hoehn M. Facilitation of electric forepaw stimulation-induced somatosensory activation in rats by additional acoustic stimulation: An fMRI investigation. *Magn. Reson. Med.* 2000; **44**(2): 317–321.
12. Lee SP, Silva AC, Ugurbil K, Kim SG. Diffusion-weighted spin-echo fMRI at 9.4 T: microvascular/tissue contribution to BOLD signal changes. *Magn. Reson. Med.* 1999; **42**(5): 919–928.
13. Lahti KM, Ferris CF, Li FH, Sotak CH, King JA. Imaging brain activity in conscious animals using functional MRI. *J. Neurosci. Meth.* 1998; **82**(1): 75–83.
14. Yang XJ, Renken R, Hyder F, Siddeek M, Greer CA, Shepherd GM, Shulman RG. Dynamic mapping at the laminar level of odor-elicited responses in rat olfactory bulb by functional MRI. *Proc. Natl Acad. Sci. USA* 1998; **95**(13): 7715–7720.
15. Mandeville JB, Marota JJ, Kosofsky BE, Keltner JR, Weissleder R, Rosen BR, Weisskoff RM. Dynamic functional imaging of relative cerebral blood volume during rat forepaw stimulation. *Magn. Reson. Med.* 1998; **39**(4): 615–624.
16. Bock C, Schmitz B, Kerskens CM, Gyngell ML, Hossmann KA, Hoehn-Berlage M. Functional MRI of somatosensory activation in rat: Effect of hypercapnic up-regulation on perfusion- and BOLD-imaging. *Magn. Reson. Med.* 1998; **39**(3): 457–461.
17. Yang X, Hyder F, Shulman RG. Functional MRI BOLD signal coincides with electrical activity in the rat whisker barrels. *Magn. Reson. Med.* 1997; **38**(6): 874–877.
18. Yang XJ, Hyder F, Shulman RG. Activation of single whisker barrel in rat brain localized by functional magnetic resonance imaging. *Proc. Natl Acad. Sci. USA* 1996; **93**(1): 475–478.
19. Hendrick RE, Raff U. Image contrast and noise. In *Magnetic Resonance Imaging*, 2nd ed, Vol. 1, Stark DD, Bradley WG. (eds). Mosby-Year Book: St Louis, MO, 1992; 109–144.
20. Kennan RP, Scanley BE, Gore JC. Physiologic basis for BOLD MR signal changes due to hypoxia/hyperoxia: Separation of blood volume and magnetic susceptibility effects. *Magn. Reson. Med.* 1997; **37**(6): 953–956.
21. Cox RW, Hyde JS. Software tools for analysis and visualization of fMRI data. *NMR Biomed.* 1997; **10**(4–5): 171–178.
22. Bandettini PA, Jesmanowicz A, Wong EC, Hyde JS. Processing strategies for time-course data sets in functional mri of the human brain. *Magn. Reson. Med.* 1993; **30**(2): 161–173.
23. Menon RS, Ogawa S, Tank DW, Ugurbil K. 4 Tesla gradient recalled echo characteristics of photic stimulation-induced signal changes in the human primary visual-cortex. *Magn. Reson. Med.* 1993; **30**(3): 380–386.
24. Yang QX, Smith MB, Briggs RW, Rycyna RE. Microimaging at 14 tesla using GESEPI for removal of magnetic susceptibility artifacts in  $T_2^*$ -weighted image contrast. *J. Magn. Reson.* 1999; **141**(1): 1–6.
25. van Zijl PCM, Eleff SM, Ulatowski JA, Oja JME, Ulug AM, Traystman RJ, Kauppinen RA. Quantitative assessment of blood flow, blood volume and blood oxygenation effects in functional magnetic resonance imaging. *Nat. Med.* 1998; **4**(2): 159–167.
26. Wood ML, Bronskill MJ, Mulkern RV, Santyr GE. Physical MR desktop data. *J. Magn. Reson. Imag.* 1993; **3**(S): 19–24.
27. Callaghan PT. Principles of Magnetic Resonance Microscopy. Oxford University Press: New York, 1991.
28. Ogawa S, Menon RS, Tank DW, Kim SG, Merkle H, Ellermann JM, Ugurbil K. Functional brain mapping by blood oxygenation level-dependent contrast magnetic-resonance-imaging—a comparison of signal characteristics with a biophysical model. *Biophys. J.* 1993; **64**(3): 803–812.
29. Huang W, Plyka I, Li H, Eisenstein EM, Volkow ND, Springer CS Jr. Magnetic resonance imaging (MRI) detection of the murine brain response to light: temporal differentiation and negative functional MRI changes. *Proc. Natl Acad. Sci. USA* 1996; **93**(12): 6037–6042.
30. Woolsey TA, Van der Loos H. The structural orientation of layer IV in the somatosensory region (SI) of mouse cerebral cortex: the description of a cortical field composed of discrete cytoarchitectonic units. *Brain Res.* 1970; **17**: 205–242.
31. Wallace MN. Histochemical-demonstration of sensory maps in the rat and mouse cerebral-cortex. *Brain Res.* 1987; **418**(1): 178–182.
32. Ogawa S, Lee TM, Nayak AS, Glynn P. Oxygenation-sensitive contrast in magnetic-resonance image of rodent brain at high magnetic-fields. *Magn. Reson. Med.* 1990; **14**(1): 68–78.
33. Gati JS, Menon RS, Ugurbil K, Rutt BK. Experimental determination of the BOLD field strength dependence in vessels and tissue. *Magn. Reson. Med.* 1997; **38**(2): 296–302.
34. Malonek D, Dirnagl U, Lindauer U, Yamada K, Kanno I, Grinvald A. Vascular imprints of neuronal activity: relationships between the dynamics of cortical blood flow, oxygenation, and volume changes following sensory stimulation. *Proc. Natl Acad. Sci. USA* 1997; **94**(26): 14826–14831.
35. Kim DS, Duong TQ, Kim SG. High-resolution mapping of iso-orientation columns by fMRI. *Nat. Neurosci.* 2000; **3**(2): 164–169.
36. Hennig J, Nauerth A, Friedburg H. Rare imaging—a fast imaging method for clinical MR. *Magn. Reson. Med.* 1986; **3**(6): 823–833.
37. Grieve SM, Blamire AM, Styles P. The effect of bulk susceptibility on murine snapshot imaging at 7.0 T: A comparison of snapshot imaging techniques. *Magn. Reson. Med.* 2000; **43**(5): 747–755.
38. Silva AC, Williams DS, Koretsky AP. Evidence for the exchange of arterial spin-labeled water with tissue water in rat brain from diffusion-sensitized measurements of perfusion. *Magn. Reson. Med.* 1997; **38**(2): 232–237.
39. Lindauer U, Villringer A, Dirnagl U. Characterization of cbf response to somatosensory stimulation-model and influence of anesthetics. *Am. J. Physiol.* 1993; **264**(4): H1223–H1228.
40. Paxinos G. The Rat Nervous System. Academic Press: Sydney, 1985.